

Crystallization of the *Bacillus subtilis* RTP–DNA complex prepared using NMR spectroscopyJulian P. Vivian,^a Jackie A. Wilce,^b Adam F. Hastings^c and Matthew C. J. Wilce^{a*}^aDepartment of Pharmacology/Crystallography Centre, University of Western Australia and the

Western Australian Institute for Medical Research, Nedlands, WA 6907, Australia,

^bDepartment of Chemistry/Biochemistry, University of Western Australia and the Western Australian Institute for Medical Research, Nedlands, WA 6907, Australia, and^cDepartment of Biochemistry, University of Sydney, NSW 2006, Australia

Correspondence e-mail:

mwilce@receptor.pharm.uwa.edu.au

The replication terminator protein (RTP)–DNA complex of *Bacillus subtilis* is responsible for the arrest of DNA replication at terminator sites in the *B. subtilis* chromosome. The crystallization and preliminary diffraction data analysis for the complex of an ¹⁵N-labelled mutant form of RTP and a symmetrical form of its DNA-binding site is reported. NMR spectroscopy was used to assess the stoichiometry of complex formation, with the sample containing the most homogenous solution of complex giving rise to diffracting crystals. Synchrotron-radiation data to 2.5 Å were collected from a crystal of space group *P*3₂21, unit-cell parameters $a = b = 44.780$, $c = 395.582$ Å, containing an RTP dimer within the asymmetric unit.

Received 15 September 2000

Accepted 4 December 2000

1. Introduction

The coordinated termination of DNA replication is an important step in the life cycle of bacteria with circular chromosomes, but has only been defined at a molecular level in two systems to date, *Escherichia coli* and *B. subtilis* (Hill, 1996; Wake, 1997). Replication of the *E. coli* and *B. subtilis* chromosomes is initiated at a specific replication ‘origin’ from where replication forks migrate bidirectionally until they meet and fuse in a restricted ‘terminus’ region located opposite the origin. This is effected by terminator proteins which bind to specific terminator (Ter) sites and halt the progress of the replicative machinery in a directional manner. Whilst the *E. coli* termination system has been structurally characterized (Kamada *et al.*, 1996), the structure of the replication terminator protein (RTP) of *B. subtilis* bound to its cognate DNA has so far eluded researchers.

In *B. subtilis*, each Ter site is a 30 bp DNA sequence comprised of two imperfect inverted repeats which overlap at a trinucleotide sequence (Lewis *et al.*, 1990). Each of these sites, named *A* and *B*, is capable of binding one dimer of RTP. The *B* site has a higher affinity for RTP, with cooperative binding occurring at the *A* site once the *B* site is filled (Langley *et al.*, 1993; Smith *et al.*, 1996). The replication fork is blocked when it approaches the Ter sequence proximal to the *B* site. However, when it approaches from the *A* site it is able to pass unimpeded through the terminator complex (Griffiths & Wake, 2000). The structural basis of this polar replication fork arrest has not yet been shown and has been the subject of much debate (Manna, Pai, Bussiére, Davies *et al.*, 1996; Manna, Pai, Bussiére, White *et al.*, 1996; Duggin *et al.*, 1999).

Crystallographic studies of the 29 kDa apo RTP molecule have revealed that RTP is a symmetric homodimeric member of the ‘winged-helix’ family of DNA-binding proteins (Bussiére *et al.*, 1995; Brennan, 1993; Gajiwala & Burley, 2000). This has enabled the RTP–DNA complex to be modelled (Swindells, 1995); however, attempts to crystallize the RTP–DNA complex have so far been unsuccessful, so that the precise mode of binding of RTP to its cognate DNA-binding site is not known.

In this study, nuclear magnetic resonance (NMR) spectroscopy has been used to monitor the titration of a symmetric *B*-site DNA into a solution of mutant RTP. The end-point of the titration was detected when only cross-peaks arising from RTP in complex were observed. Here, we report the preparation of this novel RTP–DNA complex which resulted in the formation of diffraction-quality crystals. The structure of this complex is expected to provide important insights into the mechanism of replication fork arrest in *B. subtilis*.

2. Materials and methods

2.1. Protein preparation

An RTP-C110S mutant was utilized for its improved solubility whilst maintaining a similar DNA-binding affinity and an unperturbed tertiary structure compared with wild-type RTP. These were assessed using gel-mobility shift assays (Smith *et al.*, 1996; Duggin *et al.*, 1999) to determine the apparent Ter site K_d , analytical ultracentrifugation to determine the RTP dimer-association constant and circular dichroism and NMR spectroscopy to establish the similarity of secondary and tertiary structure (unpublished results).

¹⁵N-labelled samples of RTP-C110S were overexpressed in *E. coli* BL21(DE3)pLysS using a pET-3 derived vector in minimal medium supplemented with vitamins and trace metals and with ¹⁵NH₄Cl as the sole nitrogen source. The protein was expressed and purified by the method of Kralicek *et al.* (1993), except that dithiothreitol was excluded from all buffers. Approximately 20 mg yields of purified protein were obtained from 500 ml of culture.

2.2. DNA preparation

The sRB oligonucleotides (srb-1: 5'-CTA TGA ACA TAA TGT TCA TAG-3'; srb-2: 5'-CTA TGA ACA TTA TGT TCA TAG-3') were purchased from Beckman Instruments (Gladesville, NSW) in crude form and were purified using reverse-phase HPLC. The purified single-stranded oligonucleotides were annealed at an equimolar concentration of 250 μM in 1 ml volumes by heating to 368 K for 5 min followed by slow cooling to 318 K. The reactions were held at 318 K for 2 h to allow annealing to occur and were subsequently cooled rapidly to 253 K. The

annealed oligonucleotides were purified by ion-exchange chromatography using a Pharmacia HR 5/5 MonoQ column.

2.3. Complex formation using NMR spectroscopy

NMR spectroscopy was used to track the formation of the protein–DNA complex. ¹⁵N-labelled RTP-C110S and duplex sRB were dialysed into 10 mM sodium phosphate buffer pH 6.0 containing 500 mM NaCl, 100 μM ethylene diamine tetraacetic acid (EDTA) and 25 μM chloramphenicol. Protein and DNA were combined in 4:1, 2:1, 1:1 and ~1:1.2 ratios (according to estimates of their concentrations using absorbance measurements at 280 and 260 nm, respectively) in 10 ml volumes and concentrated to 500 μl to obtain solutions containing 450 μM protein. D₂O was added to 5% and 3-trimethylsilyl (2,2,3,3-²H)-propionate (*d*₄-TSP) and 4-(2-aminoethyl)benzene sulfonyl fluoride (AEBSF) were added to final concentrations of 50 and 100 μM, respectively. 2D heteronuclear single quantum coherence (HSQC) spectra were

Table 1
Data-collection statistics.

Space group	<i>P</i> 3 ₂ 21
Unit-cell parameters (Å)	<i>a</i> = <i>b</i> = 44.78, <i>c</i> = 395.58
Resolution of data (Å)	2.5
Measured reflections	147110
No. of unique reflections	15166
<i>I</i> / σ	12.6 (5.2)
Redundancy	9.7
Completeness (%)	87.9 (54.2)
<i>R</i> _{sym} (%)	7.3 (17.5)

recorded at 298 K using a Bruker 600 MHz instrument for each protein–DNA preparation (Fig. 1). The protein–DNA complex solution prepared in the ~1:1.2 ratio was used without adjustment for crystallization trials.

2.4. Crystallization

Initial crystallization experiments were based on the sparse-matrix sampling method (Jancarik & Kim, 1991) using Crystal Screen I purchased from Hampton Research (USA). All crystallization trials utilized the hanging-drop vapour-diffusion method and were conducted at 293 K. Several crystallization conditions gave rise to small crystals. Fine sampling of these conditions yielded several crystal forms of a suitable size for X-ray diffraction analysis, of which one has been characterized. These crystals grew to maximum dimensions of 0.6 × 0.2 × 0.01 mm in 3 d from a mixture of 1 μl protein solution and 1 μl reservoir solution above a reservoir consisting of 2–7% PEG 4000, 0.075–0.100 M sodium acetate pH 4.6 (Fig. 2).

2.5. Data collection and processing

For cryogenic experiments, the crystals were passed through a solution of mother liquor plus 20% glycerol prior to flash-cooling. X-ray data were collected from a single native crystal at 100 K at beamline 14BMC of the Advanced Photon Source, Argonne National Laboratories. The wavelength of the synchrotron radiation was 1.00 Å and data were recorded on a Q4 CCD detector at a distance of 250 mm from the crystal (Fig. 3). The data were processed using *DENZO* and merged with *SCALEPACK* (Otwinowski & Minor, 1997). Data-collection statistics are summarized in Table 1. The completeness of the data is limited in the highest resolution bin owing to the large crystal-to-detector distance required to achieve sufficient reflection separation, compounded by the collection of

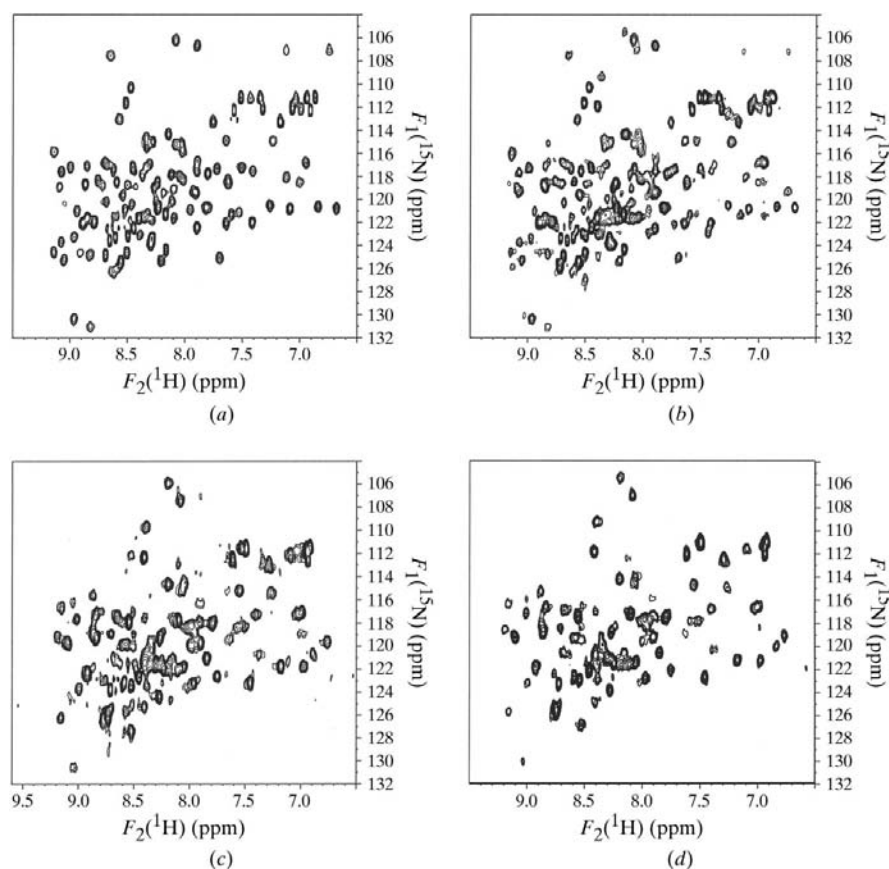


Figure 1
Region of ¹H–¹⁵N HSQC spectra acquired for RTP-C110S combined with increasing ratios of sRB: (a) shows the spectrum of RTP-C110S alone, (b) and (c) show the midpoint of the sRB titration showing cross-peaks arising from both apo and complexed RTP and (d) shows the final point of the titration in which only complexed RTP is present. This sample gave rise to the crystals used for data collection.

the diffraction data with a square-faced detector.

Molecular replacement was performed using *AMoRe* (Navaza, 1994). The search model used was a dimer generated from the crystal structure of the wild-type apo RTP solved to 2.6 Å (PDB code 1bm9) with residues 73–88 inclusive removed. Translation-function and fit-function calculations were carried out in the enantiomorphic space groups $P3_121$ and $P3_221$. The best fit-function solution $[(\theta_1, \theta_2, \theta_3) = (31.98, 91.77, 21.190), (t_x, t_y, t_z) = (0.2358, 0.6052, 0.0835)]$ was found in the $P3_221$ space group (correlation coefficient = 17.8, R factor = 52.9%). Refinement of the structure is currently in progress.



Figure 2
Crystals of the RTP-C110S-sRB complex. The plate-like crystals have approximate dimensions $0.5 \times 0.2 \times <0.01$ mm.

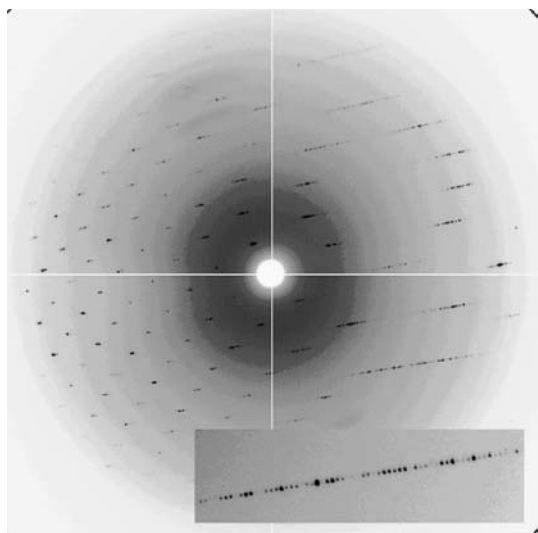


Figure 3
Diffraction image from a crystal of the RTP-C110S-sRB complex obtained using synchrotron radiation and extending to 2.5 Å resolution. The oscillation range is 1.0° and the crystal-to-film distance is 250 mm. A long c axis of 395.58 Å gives rise to the pattern shown in the insert.

3. Results and discussion

The complex between RTP and its cognate DNA-binding site in *B. subtilis* is one of only two well characterized systems known to cause DNA replication fork arrest (Wake & King, 1997). The terminator protein–DNA complex from *E. coli* has previously been structurally characterized (Kamada *et al.*, 1996), providing insight into one mechanism of polar replication fork arrest. Despite its analogous function, however, the *Bacillus* system bears no protein or DNA sequence similarity to that in *E. coli*. Its structural characterization is thus expected to provide insight into an entirely novel molecular mechanism of polar replication fork arrest.

The preparation of co-crystals of the RTP–DNA complex has, however, remained elusive until now. This may be because of several factors including the instability of RTP in solution over time, the difficulty of preparation of suitable duplex DNA and formation of the complex in an optimal stoichiometric ratio. The current study has thus employed the use of an RTP mutant in which the lone cysteine at position 110, thought to underlie a redox-state-dependent aggregation over time, has been replaced by serine, which has improved its long-term stability (unpublished results).

The DNA sequence was based on the *TerI* B site, with three changes made to make it perfectly symmetrical about its midpoint of RTP binding. This symmetrical RTP B site (sRB) encompasses the important B -site contacts utilized in the RTP-binding interaction, as determined by missing nucleotide

interference (Langley *et al.*, 1993), which extend approximately ten bases either side of the central base pair. The binding affinity was shown to be comparable with that of the B site of *TerI* (K_d values $\simeq 2 \times 10^{-11} M^{-1}$). It was also ascertained that a 21 base-pair B-form duplex DNA (~ 68 Å) would not extend beyond the known length of apo RTP (~ 85 Å in the longest direction), thus optimizing the chances of forming a compact complex structure.

The RTP–DNA complex formation was monitored by using 1H - ^{15}N HSQC spectra to observe the protein amide signals upon the addition of increasing amounts of DNA. Each 1H - ^{15}N correlation shown in the spectrum of apo RTP-

C110S (Fig. 1*a*) represents the signal arising from equivalent amides from each of the RTP-C110S subunits. Upon the addition of submolar equivalents of sRB (Figs. 1*b* and 1*c*), two sets of crosspeaks were observed representing RTP-C110S in both its apo and complexed forms. When RTP-C110S and sRB were added in the approximate molar ratio 1:1.2 the cross-peaks converged to signals arising from only the complexed RTP-C110S and were in the same number as was present for apo RTP-C110S (Fig. 1*d*), indicating that only symmetrical complexed protein was present. The high quality of the 1H - ^{15}N HSQC spectrum of the RTP-C110S-sRB complex (which is approximately 42 kDa in size) was unexpected, since molecules of this size often display considerable line broadening and poor peak intensity. It would thus appear that the complex tumbles freely in solution and does not tend to form higher molecular-weight species, which certainly would not give rise to such NMR spectra.

Whether all of these measures were necessary for the successful crystallization of the RTP–DNA complex is not known. Current studies in our laboratory now include the preparation of asymmetrical complexes of RTP-C110S with native DNA-binding sites and with longer duplex DNA preparations. The current crystal and diffraction data, however, represents an important breakthrough in the study of the RTP–DNA interaction and the molecular mechanism of replication fork arrest in *B. subtilis*.

Use of the Advanced Photon Source was supported by the US Department of Energy, Basic Energy Sciences, Office of Science under Contract No. W-31-109-Eng-38. Use of the BioCARS Sector 14 was supported by the National Institutes of Health, National Center for Research Resources under grant number RR07707. This research was supported by grants from the Arnold Yeldham and Mary Raine Medical Research Foundation (MCJW), the Australia Research Council Fellowship (JAW) and Small Grant Schemes (MCJW and JAW).

References

- Brennan, R. G. (1993). *Cell*, **74**, 773–776.
- Bussiere, D. E., Bastia, D. & White, S. W. (1995). *Cell*, **80**, 651–660.
- Duggin, I. G., Anderson, P. A., Smith, M. T., Wilce, J. A., King, G. F. & Wake, R. G. (1999). *J. Mol. Biol.* **286**, 1325–1335.
- Gajiwala, K. S. & Burley, S. K. (2000). *Curr. Opin. Struct. Biol.* **10**, 110–116.
- Griffiths, A. A. & Wake, R. G. (2000). *J. Bacteriol.* **182**, 1448–1451.

- Hill, T. M. (1996). *Escherichia Coli and Salmonella: Cellular and Molecular Biology*, edited by F. C. Neidhardt, R. Curtiss III, J. L. Ingraham, E. C. Lin, K. B. Low, B. Magasanik, W. S. Reznikoff, M. Riley, M. Schaechter & H. E. Umbarger, pp. 1602–1614. Washington, DC: American Society for Microbiology.
- Jancarik, J. & Kim, S.-H. (1991). *J. Appl. Cryst.* **24**, 409–411.
- Kamada, K., Horiuchi, T., Ohsumi, K., Shimamoto, N. & Morikawa, K. (1996). *Nature (London)*, **383**, 598–603.
- Kralicek, A. V., Vesper, N. A., Ralston, G. B., Wake, R. G. & King, G. F. (1993). *Biochemistry*, **32**, 10216–10223.
- Langley, D. B., Smith, M. T., Lewis, P. J. & Wake, R. G. (1993). *Mol. Microbiol.* **10**, 771–779.
- Lewis, P. J., Ralston, G. B., Christopherson, R. I. & Wake, R. G. (1990). *J. Mol. Biol.* **214**, 73–84.
- Manna, A. C., Pai, K. S., Bussiere, D. E., Davies, C., White, S. W. & Bastia, D. (1996). *Cell*, **87**, 881–891.
- Manna, A. C., Pai, K. S., Bussiere, D. E., White, S. W. & Bastia, D. (1996). *Proc. Natl Acad. Sci. USA*, **93**, 3253–3258.
- Navaza, J. (1994). *Acta Cryst.* **A50**, 157–163.
- Otwinowski, Z. & Minor, W. (1997). *Methods Enzymol.* **276**, 307–326.
- Smith, M. T., de Vries, C. J., Langley, D. B., King, G. F. & Wake, R. G. (1996). *J. Mol. Biol.* **260**, 54–69.
- Swindells, M. B. (1995). *Trends Biochem. Sci.* **20**, 300–302.
- Wake, R. G. (1997). *FEMS Microbiol. Lett.* **153**, 247–254.
- Wake, R. G. & King, G. F. (1997). *Structure*, **5**, 1–5.